**Estimates of red tide mortality on red grouper, 2002-2022, from the West Florida Shelf Fisheries Ecosystem Model**

A working paper for the SEDAR 88 stock assessment of Gulf of Mexico red grouper

David Chagaris
University of Florida

20 Feb 2025

## Red tide mortality estimates

Red tide mortality was estimated for reg grouper ages 0-5+ using the West Florida Shelf Fisheries Ecosystem Model (WFS-FEM), following the methods described below, in gag SEDAR72-WP01, and in Vilas et al. (2023). A few updates were made to the model since SEDAR72-WP01, primarily to stay current with biomass and fishing mortality rates from the latest stock assessments available. In addition, a calibration procedure was attempted in Ecospace to improve spatial and temporal predictions for red grouper, resulting in changes to a few predator-prey vulnerability parameters and depth preference functions. However, the calibration procedure did not produce noticeably better fits to the data and will require further development and testing.

The red tide mortality index was developed by summing the predicted red tide loss over all grid cells and monthly timesteps and dividing by the average annual biomass (by age or all ages combined), to produce an instantaneous rate of red tide mortality that can be used in stock assessment models. For all ages combined, red tide mortality was highest in 2005 (Mrt=0.531) followed by 2006 (Mrt=0.117), and 2018 (Mrt=0.104) (Table 1,Figure 1. Age-specific and population-wide estimates of red tide mortality from 2002-2022 from the WFS-FEM.Figure 1). In most years, red tide mortality was highest for the younger age stanzas that are distributed closer to shore where red tides are most severe.

Table 1. Age-specific estimates of red tide mortality on red grouper for 2002-2022 from the WFS-FEM.

| Year | age-0 | age-1 | age-2 | age-3 | age-4 | age-5+ | all ages |
|---|---|---|---|---|---|---|---|
| 2002 | 0.002 | 0.003 | 0.004 | 0.004 | 0.006 | 0.003 | 0.003 |
| 2003 | 0.020 | 0.016 | 0.016 | 0.018 | 0.013 | 0.011 | 0.012 |
| 2004 | 0.002 | 0.002 | 0.002 | 0.002 | 0.000 | 0.000 | 0.001 |
| 2005 | 0.553 | 0.569 | 0.563 | 0.598 | 0.529 | 0.520 | 0.531 |
| 2006 | 0.435 | 0.278 | 0.236 | 0.241 | 0.131 | 0.081 | 0.117 |
| 2007 | 0.012 | 0.016 | 0.029 | 0.041 | 0.038 | 0.019 | 0.024 |
| 2008 | 0.000 | 0.000 | 0.000 | 0.000 | 0.000 | 0.000 | 0.000 |
| 2009 | 0.006 | 0.008 | 0.008 | 0.010 | 0.018 | 0.008 | 0.010 |
| 2010 | 0.000 | 0.000 | 0.000 | 0.000 | 0.000 | 0.000 | 0.000 |
| 2011 | 0.044 | 0.045 | 0.045 | 0.053 | 0.077 | 0.054 | 0.056 |
| 2012 | 0.134 | 0.087 | 0.066 | 0.071 | 0.070 | 0.037 | 0.049 |
| 2013 | 0.010 | 0.002 | 0.001 | 0.002 | 0.001 | 0.001 | 0.001 |
| 2014 | 0.012 | 0.015 | 0.018 | 0.022 | 0.035 | 0.028 | 0.027 |
| 2015 | 0.048 | 0.059 | 0.063 | 0.067 | 0.063 | 0.056 | 0.059 |

| Year | age-0 | age-1 | age-2 | age-3 | age-4 | age-5+ | all ages |
|---|---|---|---|---|---|---|---|
| 2016 | 0.057 | 0.047 | 0.034 | 0.023 | 0.011 | 0.010 | 0.014 |
| 2017 | 0.005 | 0.006 | 0.006 | 0.007 | 0.006 | 0.002 | 0.003 |
| 2018 | 0.162 | 0.159 | 0.124 | 0.118 | 0.140 | 0.092 | 0.104 |
| 2019 | 0.152 | 0.071 | 0.043 | 0.034 | 0.037 | 0.025 | 0.029 |
| 2020 | 0.084 | 0.006 | 0.000 | 0.000 | 0.000 | 0.000 | 0.000 |
| 2021 | 0.098 | 0.107 | 0.083 | 0.054 | 0.050 | 0.036 | 0.044 |
| 2022 | 0.231 | 0.198 | 0.187 | 0.126 | 0.088 | 0.068 | 0.087 |

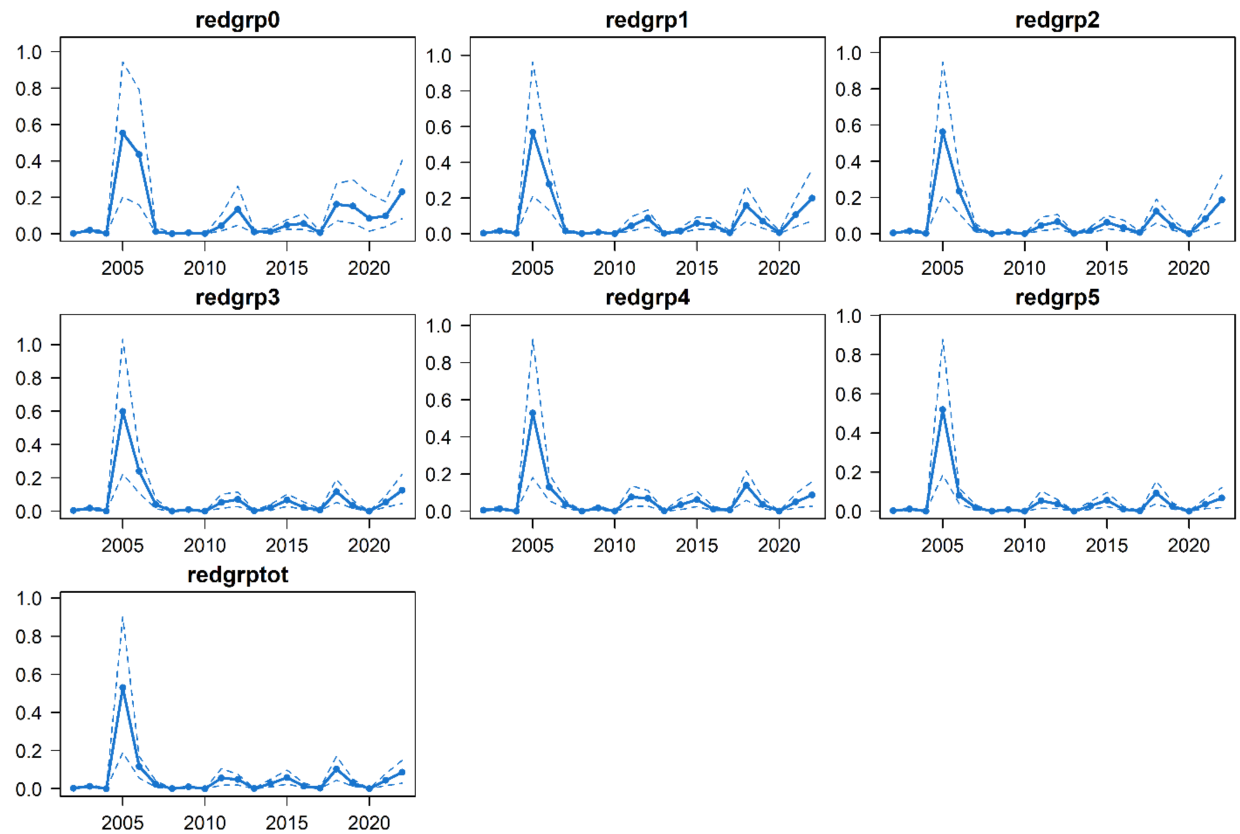


Figure 1. Age-specific and population-wide estimates of red tide mortality from 2002-2022 from the WFS-FEM.

### Red tide age-based selectivity

To inform selectivity of the red tide fleet in the SEDAR88 stock assessment model, we rescaled the red tide mortality to the maximum value across ages for each year, and provided those vectors for the years under consideration 2005, 2006, 2014, 2018, and 2021. In years 2006, 2018, and 2021 there is a general decline in selectivity with age, as these were nearshore events impacting the youngest age stanzas. Selectivity is fairly constant across age in 2005 when the red tide bloom extended offshore over a large portion of the West Florida Shelf. In contrast, the 2014 bloom was an isolated patch offshore in the Big Bend region that impacted older ages, and therefore exhibits higher selectivity for older ages in that year.

Table 2. Red tide selectivity at age derived from mortality estimates for 5 years under consideration for inclusion in the stock assessment model.

| Age | y2005 | y2006 | y2014 | y2018 | y2021 |
|---|---|---|---|---|---|
| 0 | 0.924 | 1.000 | 0.342 | 1.000 | 0.916 |
| 1 | 0.951 | 0.639 | 0.422 | 0.976 | 1.000 |
| 2 | 0.940 | 0.541 | 0.516 | 0.764 | 0.776 |
| 3 | 1.000 | 0.552 | 0.623 | 0.725 | 0.507 |
| 4 | 0.884 | 0.301 | 1.000 | 0.865 | 0.471 |
| 5+ | 0.869 | 0.186 | 0.810 | 0.568 | 0.339 |

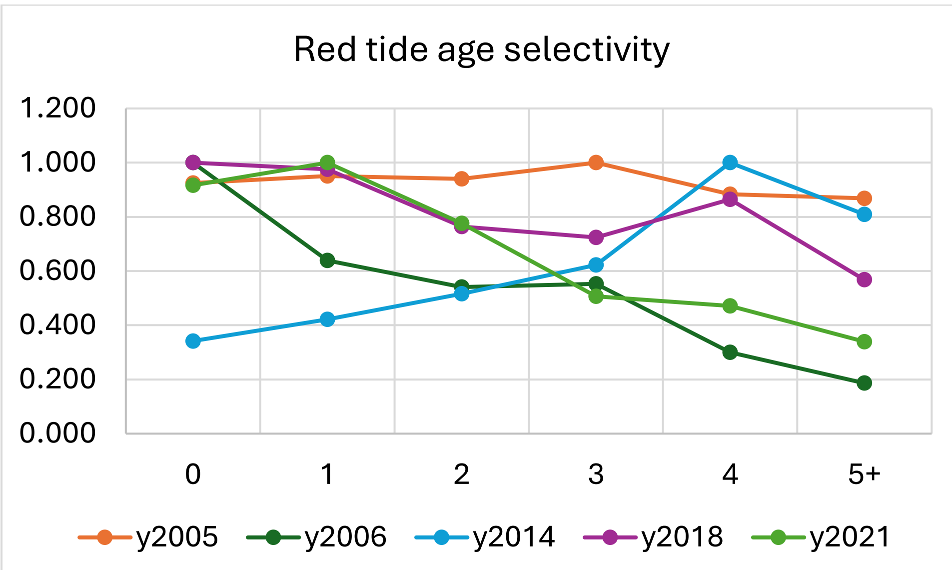


Figure 2. Red tide selectivity at age derived from mortality estimates for 5 years under consideration for inclusion in the stock assessment model.

**Methods**

***The West Florida Shelf Fisheries Ecosystem Model***

The West Florida Shelf fisheries ecosystem model (WFS-FEM) is developed using the Ecopath with Ecosim and Ecospace (EwE, Christensen and Walters 2004). The WFS-FEM simulates spatial-temporal biomass and fishing dynamics from 1985-2022 at monthly timestep over a 10-minute spatial grid. The model includes 83 functional groups and 18 fishing fleets, and focuses on reef fish species with key species separated into age stanzas. The current model was adapted from Okey et al. (2004) to screen policy options (Chagaris 2013; Chagaris et al. 2015), evaluate impacts of invasive lionfish (Chagaris et al. 2017), and incorporate red tide impacts (Vilas et al. 2023). The model is more thoroughly described in Vilas et al. (2023), archived at NCEI (https://doi.org/10.25921/t26e-wj91), and available for download at the UF repository (https://ufdc.ufl.edu/ir00011604/00001). The model was last used to estimate red tide mortality for the SEDAR 72 stock assessment of gag grouper, with an update through June 2023 provided to the SSC at its September 2023 meeting.

Partial updates were made to the model for SEDAR 88, including updating the biomass inputs and timeseries to match more recent stock assessments for a few species (available as of December 2023) and re-estimating key parameters to improve spatial and temporal dynamics.

Red grouper are included in the WFS-FEM as 6 age stanzas, going from age 0-5+, to represent ontogeny in diet, habitat, and fishery selectivity (Figure 3). The initial (1985) biomass input for the 'leading' age stanza (age 5+) was estimated to be 15,824 mt in the SEDAR 61 stock assessment, and biomass for the other ages was calculated by EwE assuming a stable age distribution. Total mortality rate (Z) inputs were also obtained from

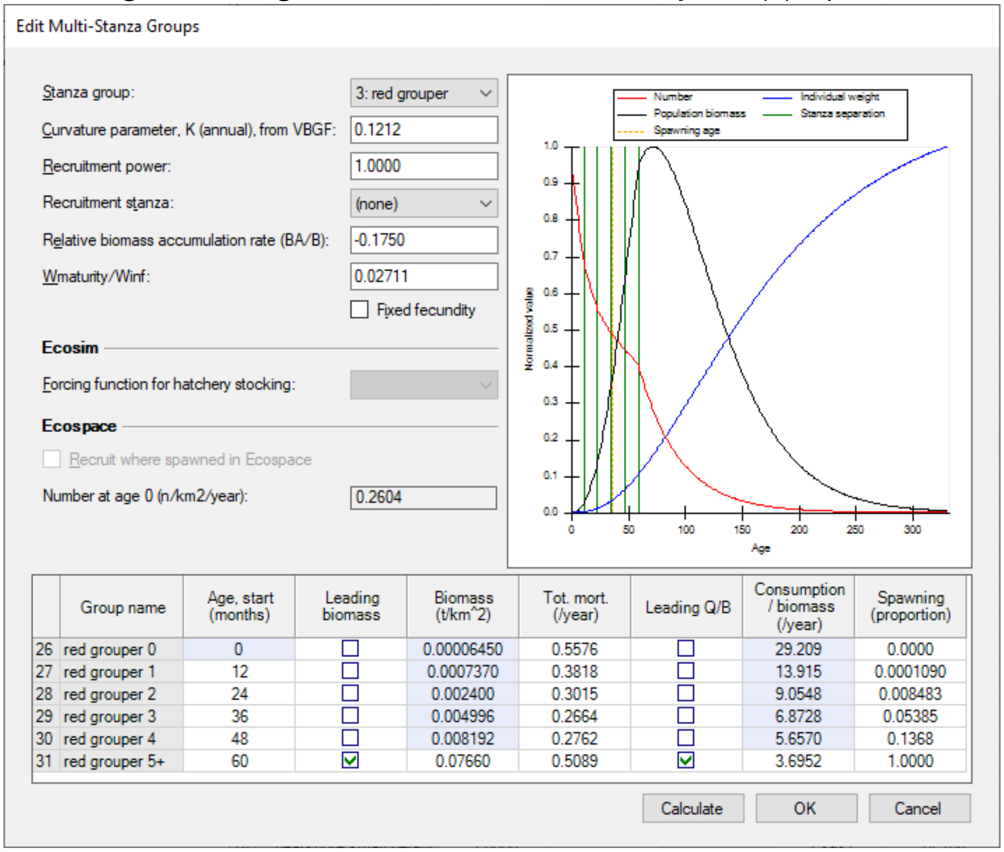


| | Group name | Age, start (months) | Leading biomass | Biomass (t/km^2) | Tot. mort. (/year) | Leading Q/B | Consumption / biomass (/year) | Spawning (proportion) |
|---|---|---|---|---|---|---|---|---|
| 26 | red grouper 0 | 0 | ☐ | 0.00006450 | 0.5576 | ☐ | 29.209 | 0.0000 |
| 27 | red grouper 1 | 12 | ☐ | 0.0007370 | 0.3818 | ☐ | 13.915 | 0.0001090 |
| 28 | red grouper 2 | 24 | ☐ | 0.002400 | 0.3015 | ☐ | 9.0548 | 0.008483 |
| 29 | red grouper 3 | 36 | ☐ | 0.004996 | 0.2664 | ☐ | 6.8728 | 0.05385 |
| 30 | red grouper 4 | 48 | ☐ | 0.008192 | 0.2762 | ☐ | 5.6570 | 0.1368 |
| 31 | red grouper 5+ | 60 | ☑ | 0.07660 | 0.5089 | ☑ | 3.6952 | 1.0000 |

Figure 3. WFS-FEM Ecopath mult-stanza inputs for red grouper.

SEDAR 61, and converted to biomass units used in EwE. The total natural mortality rate for red grouper declines with age according to the Lorenzen function used in SEDAR 61, while fishing mortality increases with age (Figure 4). There is a large amount of unexplained mortality for red grouper in the WFS-FEM, owing to the fact that very few red grouper appear as prey items in the stomach content data. The consumption rate (Q/B) was derived from empirical equations relating fish body shape and activity to consumption rates and was determined to be 3.6952 for the age 5+ stanza and calculated for the other ages scaled to body weight raised to the power of 2/3. Diet compositions inputs for red grouper were derived from data collected by the FWC gut lab and other published studies available in the Gulf of Mexico Species Interactions Database. Red grouper are primarily invertebrate feeders until about age-3 when they start to consume more fish (Figure 5).

In Ecospace, red grouper are assigned age-specific depth preference functions and a single rugosity preference function shared by all ages (Figure 6). The depth preference functions were based on generalized additive models applied to fishery survey data (bottom longline, cameras), and demonstrate an ontogenetic shift to deeper water as fish age. The rugosity function was a generalized shape to represent preference for low-relief bottom habitat. All preference functions were described using the 2-parameter beta function option in Ecospace. The baseline dispersal rate for all red grouper age stanzas was 54 km/yr and based on tagging recapture data.

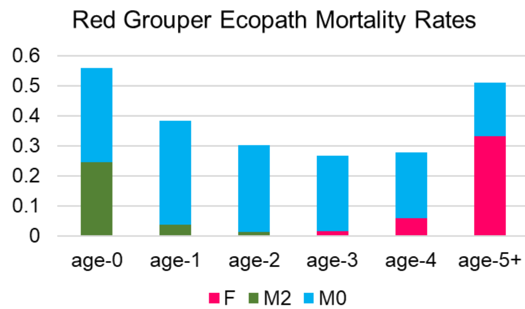


Figure 4. Total mortality rates for red grouper in the WFS-FEM Ecopath model, partitioned into fishing (F), predation (M2), and other (M0) mortality.

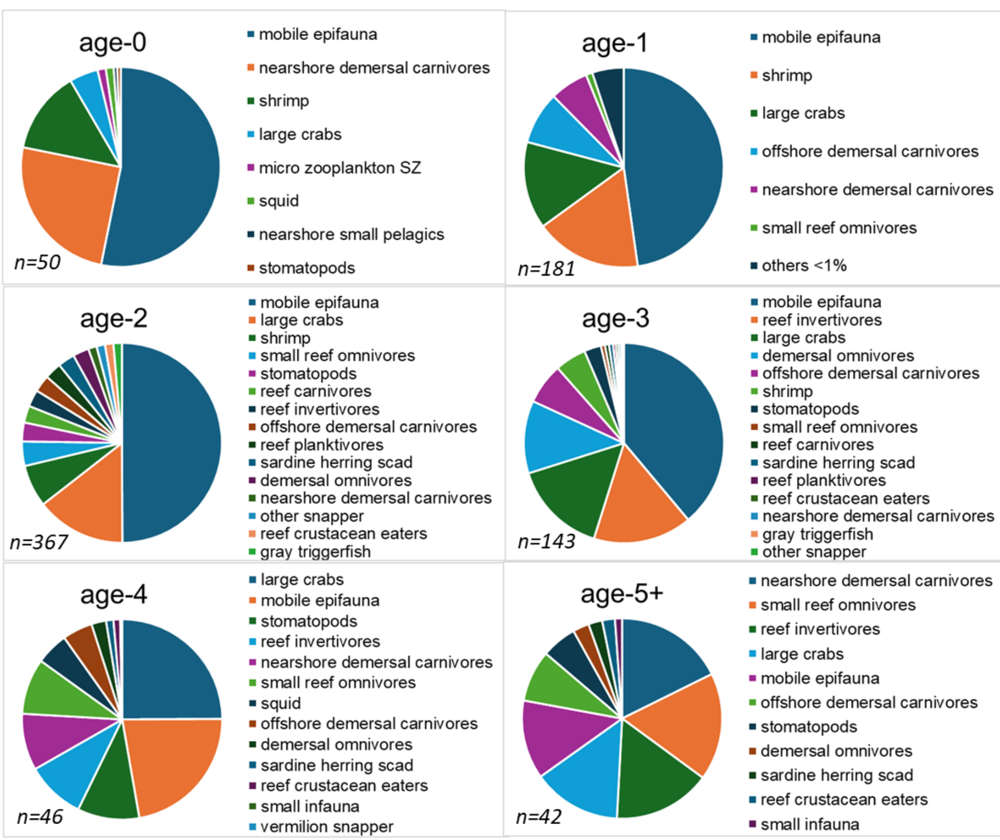


Figure 5. Input diet compositions for red grouper in the WFS-FEM.

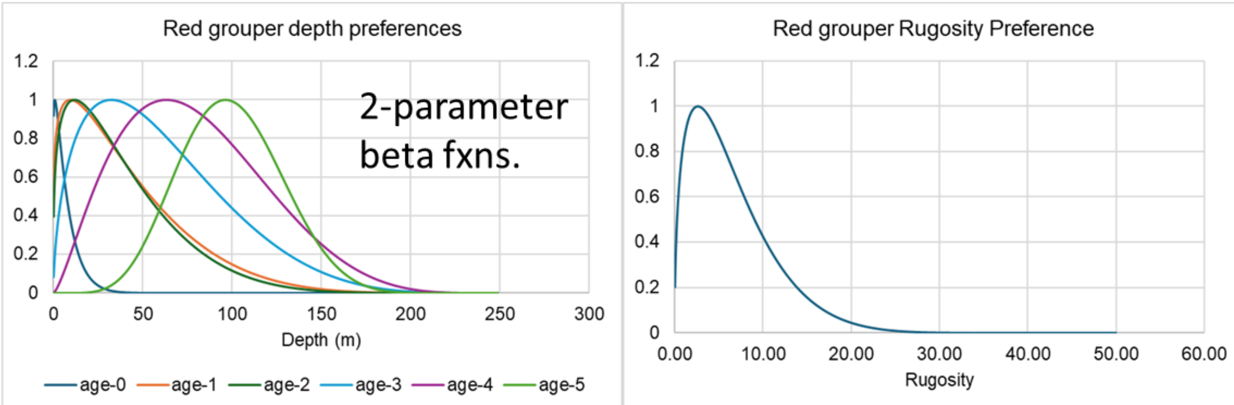

Figure 6. Depth and rugosity preference functions for red grouper used in the WFS-FEM.

***Red Tide Mortality Simulations (as described in SEDAR72-WP01)***

*Creation of Red tide maps*

*K. brevis* cell concentration (cells/L) data collected by Florida Fish and Wildlife Research Institute Harmful Algal Bloom monitoring group (FWRI-HAB) were interpolated over the entire WFS using ordinary kriging. For each month and sample location we obtained the maximum observed *K. brevis* cell concentration and performed ordinary kriging for months when there were at least 5 sites with maximum concentrations greater than or equal to 1,000 cells/L. The 'automap' [R] package (Hiemstra et al. 2009) was used to fit the variogram model to the log-transformed monthly observed maximum cell concentrations at each sample location. Several variogram model types were tested, including the commonly used spherical, exponential, and matern (M. Stein's parameterization) models, and the model with the smallest residual sum of squares in the sample variogram was selected. The selected model and data were used to predict cell concentrations over a spatial grid and then back-transformed. Monthly normalized fluorescent line height (nFLH) grids derived from the MODIS-Aqua satellite (NASA Goddard Space Flight Center 2020) were used to define the spatial extent and duration of harmful algal blooms. Monthly maps of the WFS with HAB polygons were generated from nFLH based on a threshold detection value 0.02 mW cm-2 um-1 sr-1 (Hu et al., 2005) Lastly, the kriged maps were clipped to the HAB polygons and resampled to match the resolution of the Ecospace model (Figure 7). The monthly red tide concentration maps were then loaded into the Ecospace spatial-temporal framework as a time series of spatial ASCII files.

*Simulating red tides effects in Ecospace*

Red tide response functions were defined to generate direct mortality and sub-lethal effects (i.e. reduced feeding & growth, and movement) of red tides. The red tide mortality response determined the proportion of biomass killed ($P_{m,t}$) in each map cell *m* and monthly time step *t* as a function of *K. brevis* cell concentration, $x_{m,t}$. The mortality response functions assumed a logistic curve with a slope, *b,* that were computed from multiple scalar values (1,000, 20,000, 50,000 and 100,000) and multiple inflection points,

*c*, of 50,000, 100,000, 200,000, 300,000 and 400,000 cells/L, representing multiple sensitivity levels and 20 red tide mortality response functions (Figure 8,
Table 3).

$$P_{m,t} = \frac{1}{1 + \left(\frac{x_{m,t}}{c}\right)^{-b}}$$

The proportion killed in each grid cell was converted to an annual instantaneous mortality rate, $\hat{P}$ , which is used to determine the biomass killed due to red tides (*RTloss*).

$$\hat{P}_{m,t} = -\ln\left(1 - P_{m,t} * 12\right)$$

$$RTloss_{m,t} = B_{m,t} \cdot \frac{\hat{P}_{m,t}}{12}$$

An annual time series of red tide mortality was calculated by dividing the total red tide loss over all map cells and months by the average annual biomass.

$$MRT_y = \frac{\sum_{m,t} RTloss_{m,t,y}}{(\sum_{m,t} B_{m,t,y})/12}$$

For simpler integration into Ecospace and to utilize the existing 'other mortality forcing' component of the loss equation, the $\hat{P}_{m,t}$ was scaled to the Ecopath other mortality rate, *M0base*, to return the other mortality multiplier term, $M0mult_{i,t}$, for a grid cell and monthly time step.

$$M0mult_{m,t} = (\hat{P}_{m,t} + M0base)/M0base$$

For each species or FG *i* the total biomass loss in each cell and timestep was calculated as

$$loss_i = Q_i + (M0base_i * M0mult_i * ((1 - M0pred_i) + M0pred_i * FT_i) + E_i + F_i) * B_i \quad (3)$$

Where $M0pred_i$ is an input value representing the fraction of other mortality sensitive to changes in foraging time (*FT*), *E* is an emigration rate, *F* is fishing mortality, and *B* is biomass. In these scenarios, *M0pred* is zero for all groups. Predation losses are determined through foraging arena equations and fishing effort (and therefore *F*) is distributed spatially using a gravity model.

The foraging responses serve two roles in the simulations. First, they reduce the foraging arena size in affected grid cells, which thereby reduces consumption and biomass growth. Additionally, the reduced foraging capacity in an affected cell will increase the movement rate out of that cell. This allows model groups to move away from red tide blooms and may mitigate direct mortality losses if cells with suitable habitat are nearby. The red tide foraging response was defined using a logistic curve that decreased with red tide cell concentrations (Figure 8**Error! Reference source not found.**). The foraging responses had lower inflections points (from 12,500 to 300,000 cells/L) than the mortality responses since sub-lethal effects and avoidance response are likely to be experienced at lower *K. brevis* concentrations. Three foraging curves were generated for each value of *c*, at multiple sensitivity levels of 25%, 50%, and 75% of the mortality inflection point. The slope for each foraging response curve was scaled relative to the inflection point, using a multiplier of $-5e^{-5}$, such that the shape of the curve did not change, while its position on the x-axis did. This resulted in 15 foraging response functions (three foraging response curves for each mortality inflection point function) that represent multiple sensitivity levels (Figure 8).

Table 3. Set of 160 red tide scenarios evaluated with the WFS Ecospace model.

| Sensitivity (i.e. response fxns) | response applied to gag stanzas only | | response applied to all consumer groups | |
|---|---|---|---|---|
| | M0 | M0+foraging | M0 | M0+foraging |
| high | run1-run4 | run21-run32 | run81-run84 | run101-run112 |
| medium-high | run5-run8 | run33-run44 | run85-run88 | run113-run124 |
| medium | run9-run12 | run45-run56 | run89-run92 | run125-run136 |
| medium-low | run13-run16 | run57-run68 | run93-run96 | run137-run148 |
| low | run17-run20 | run69-run80 | run97-run100 | run149-run160 |

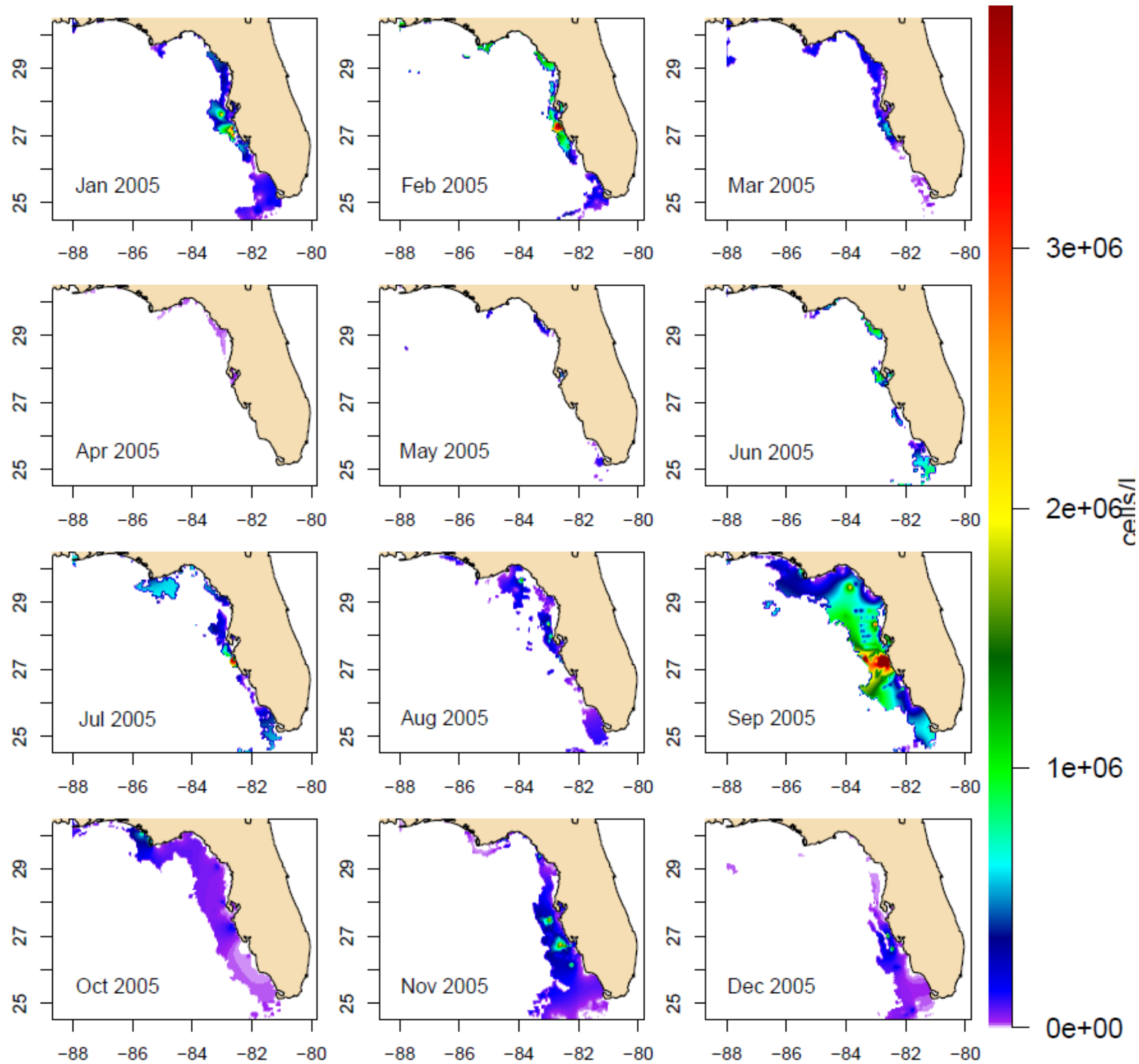


Figure 7. Red tide maps used in the WFS-FEM for 2005, 2006, 2014, 2018, 2021, and 2022.

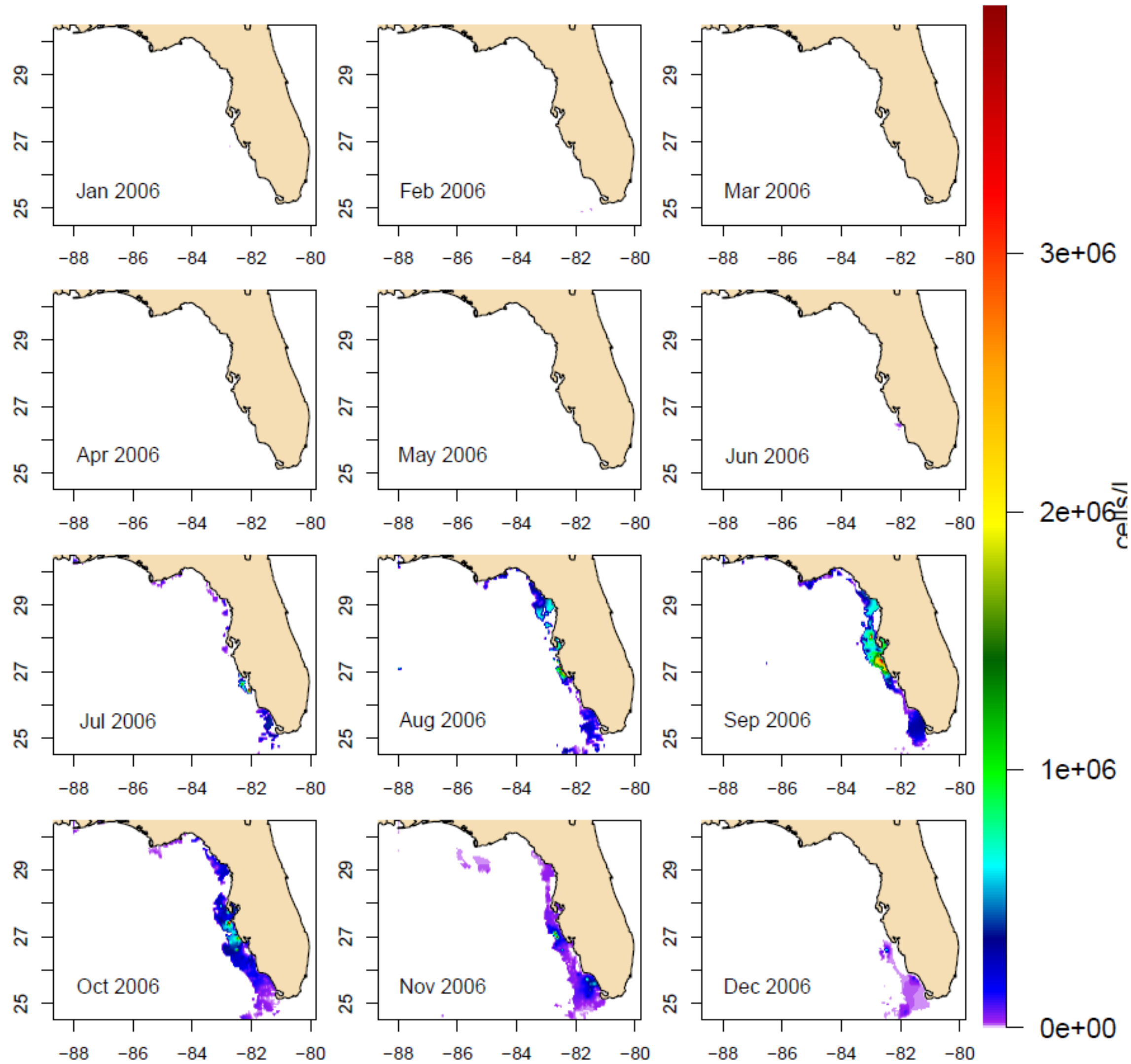


Figure 7 cont.

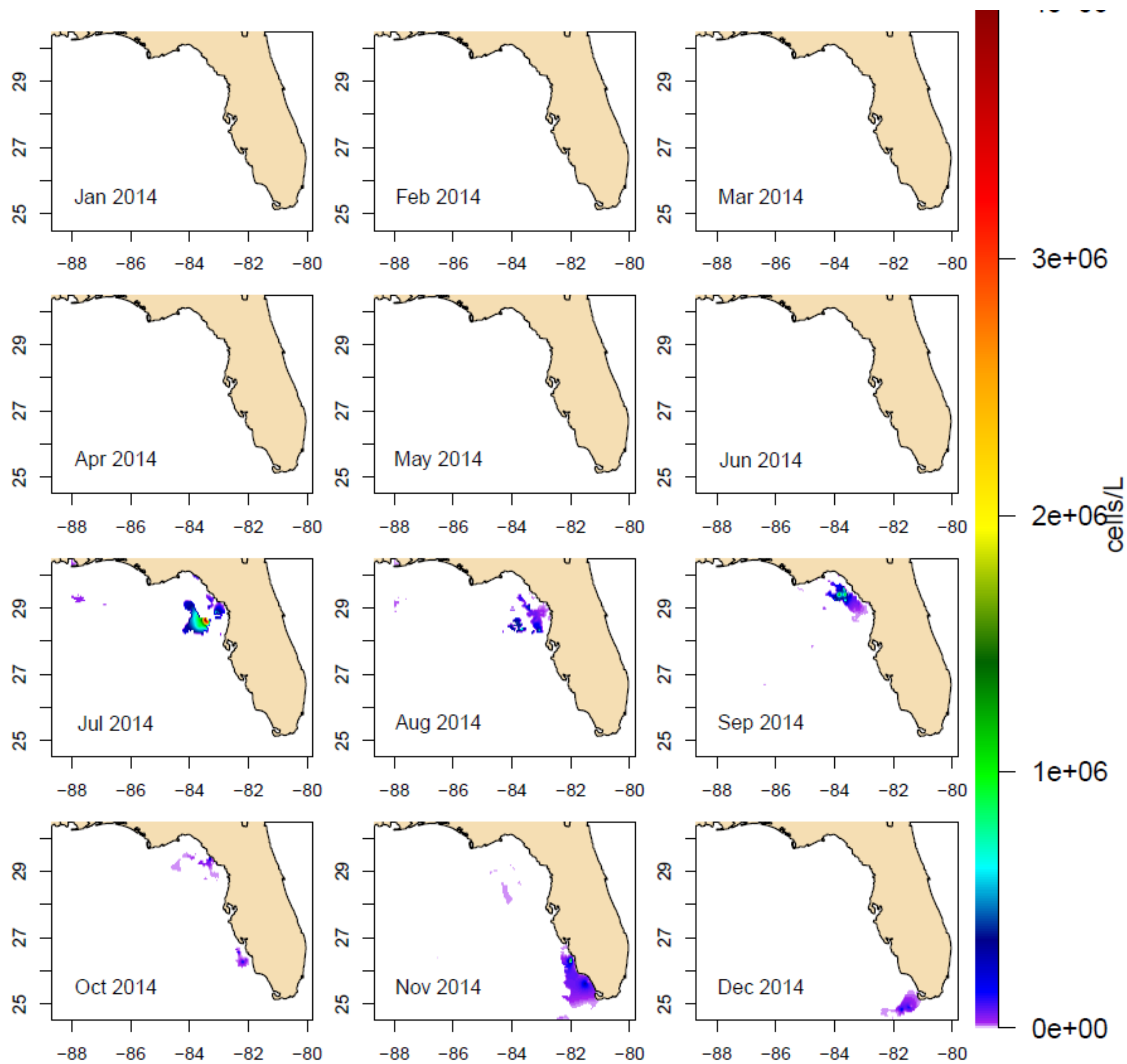


Figure 7 cont.

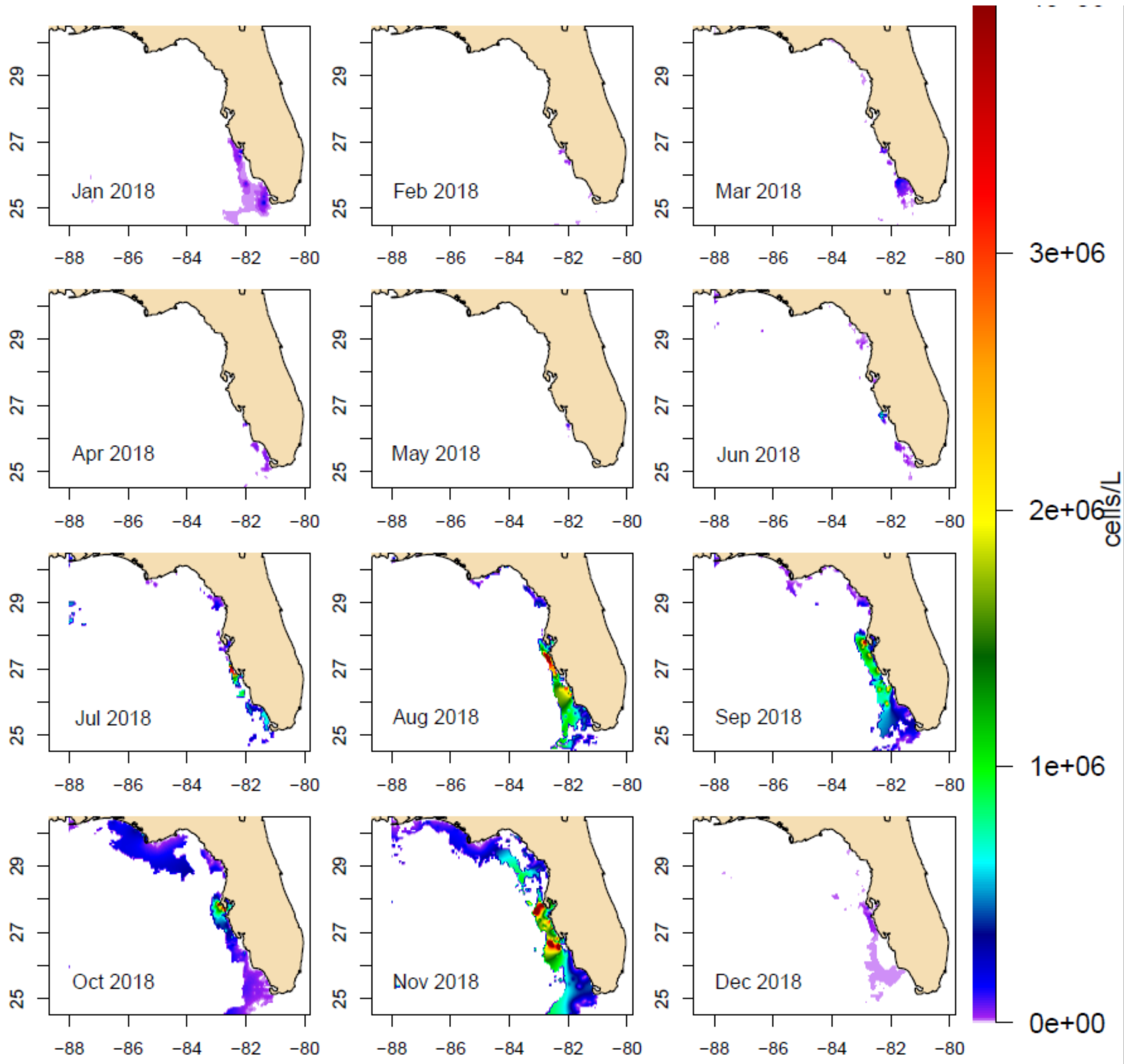


Figure 7 cont.

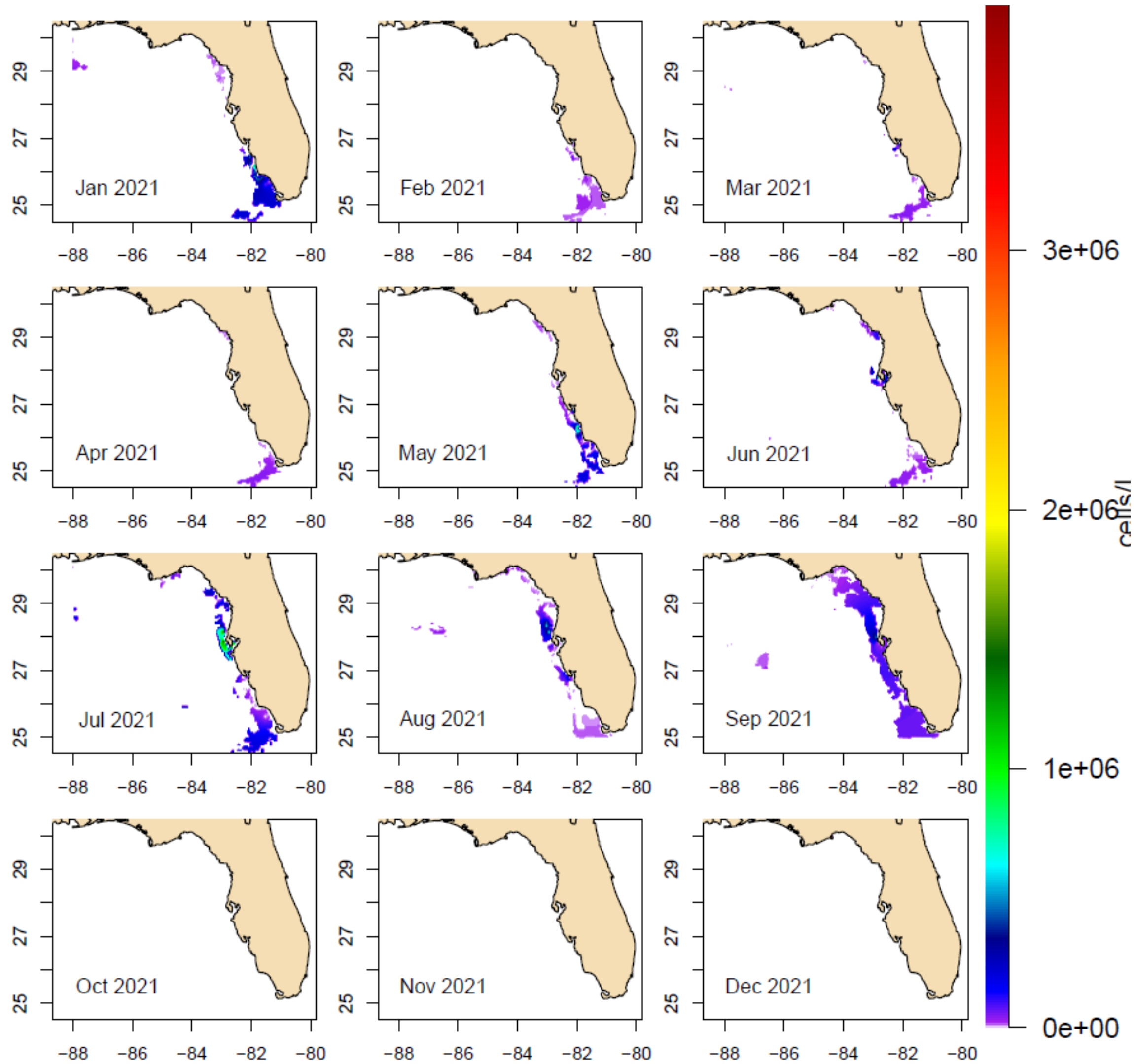


Figure 7 cont.

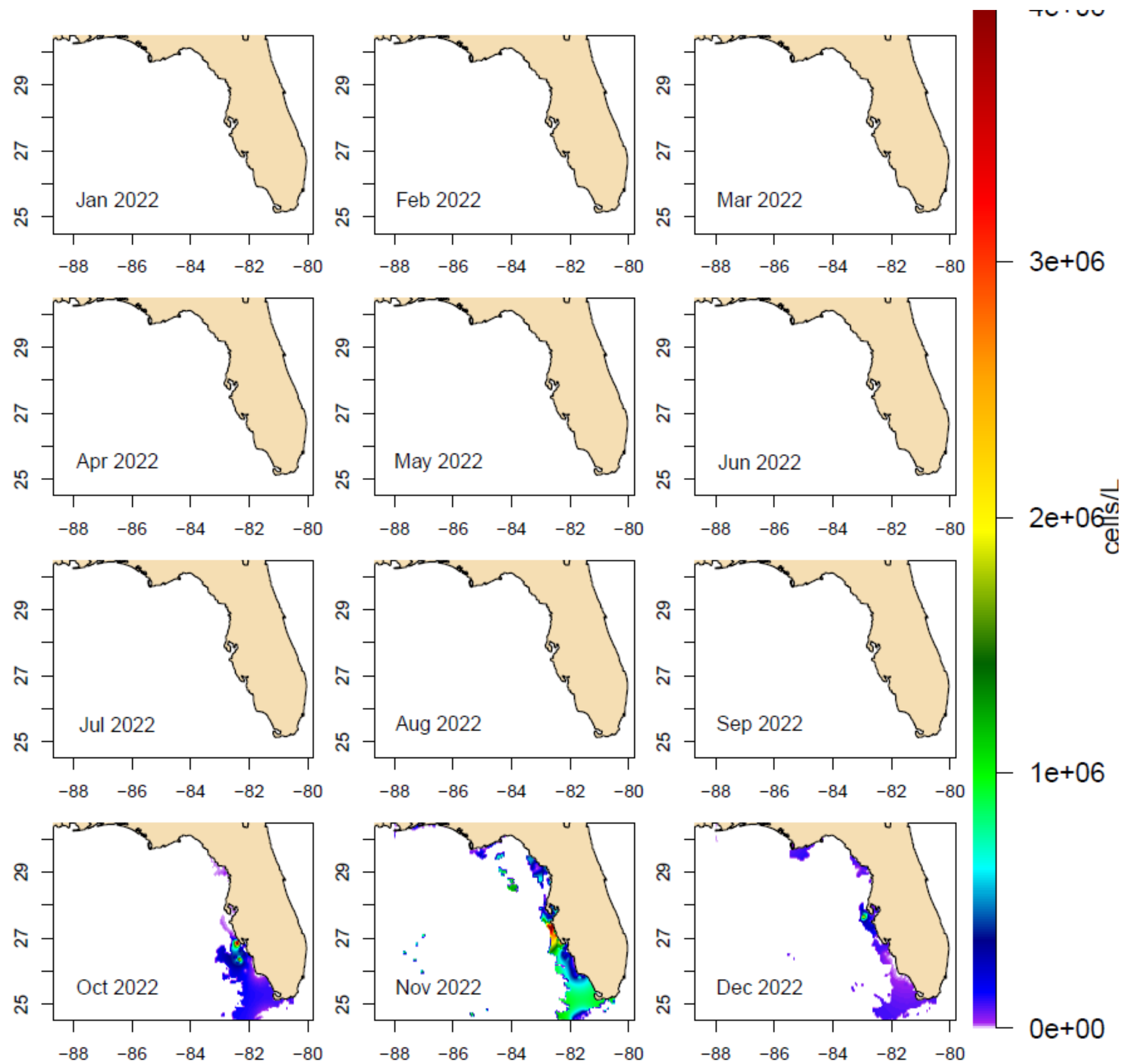


Figure 7 cont.

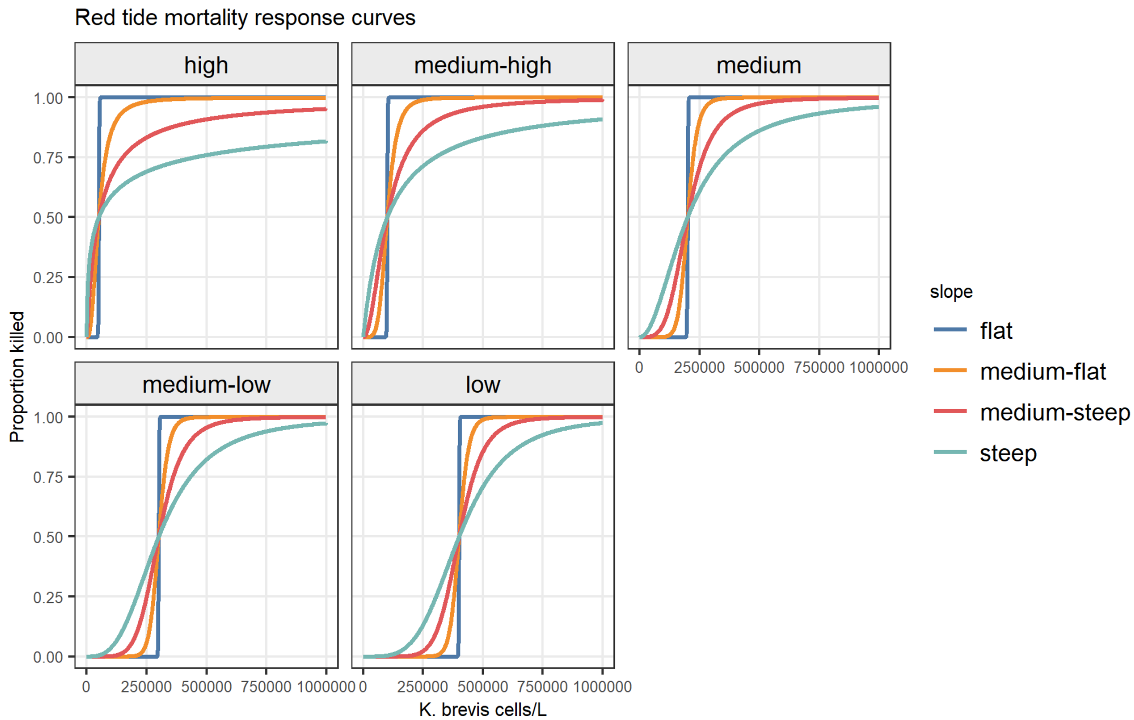


Figure 8. Lethal (left) and sub-lethal (right) red tide response curves used in the WFS-FEM.